ORIGINAL ARTICLE

Improved surgical margin definition by narrow band imaging for resection of oral squamous cell carcinoma: A prospective gene expression profiling study

Camile S. Farah, PhD,[1,2]* Andrew J. Dalley, PhD,[1] Phan Nguyen, MBBS,[3] Martin Batstone, MBBS,[1,4] Farzaneh Kordbacheh, PhD,[1] Joanna Perry–Keene, MBBS,[5] David Fielding, MBBS[6]

[1]University of Queensland Centre for Clinical Research, The University of Queensland, Brisbane, Queensland, Australia, [2]Australian Centre for Oral Oncology Research and Education, Brisbane, Queensland, Australia, [3]Department of Thoracic Medicine, Royal Adelaide Hospital, Adelaide, Australia, [4]Maxillofacial Unit, Royal Brisbane and Women's Hospital, Brisbane, Queensland, Australia, [5]Department of Pathology, Royal Brisbane and Women's Hospital, Brisbane, Queensland, Australia, [6]Department of Thoracic Medicine, Royal Brisbane and Women's Hospital, Brisbane, Queensland, Australia.

ABSTRACT: *Background.* Incomplete primary tumor excision contributes to localized postsurgical recurrence of oral squamous cell carcinoma (OSCC). The purpose of this study was to provide molecular evidence that surgical margin definition using narrow band imaging (NBI) resulted in more complete OSCC excision than conventional white light (WL) panendoscopy.

Methods. Molecular divergence among tumor, WL, and NBI-defined surgical margins was compared in 18 patients through microarray analysis (GeneChip U133-plus-2.0).

Results. The numbers of differentially expressed genes (NBI = 4387; WL = 3266; vs tumor) signified that NBI placed margins into less involved tissue than WL examination. Principal component analysis segregated tumor, WL, and NBI tissues appropriately based solely on mRNA profiles, and unsupervised hierarchical clustering identified 4 patients (22%) who benefited directly from NBI surgical margin definition. Gene ontology enrichment indicated increasing cell phenotypic diversity: tumor<WL<NBI.

Conclusion. Resection to NBI-defined margins will leave less dysplastic and malignant residual tissue and thereby increase ablative surgery success rates. © 2015 Wiley Periodicals, Inc. *Head Neck* 38: 832–839, 2016

KEY WORDS: surgical margins, oral squamous cell carcinoma, narrow band imaging, prevention of second cancers, microarray analysis

INTRODUCTION

Oral squamous cell carcinoma (OSCC) accounts for 90% of oral malignancy and is the sixth most common cancer worldwide.[1] Postsurgical reoccurrence of OSCC is commonplace either locally or at remote intraoral sites, contributing factors being field cancerization and incomplete primary tumor removal. Current best practice for ablative OSCC resection is to excise 5 mm beyond the visible cancer perimeter,[2,3] ensuring, where practical, that the surgical margin lies within nondiseased tissue. Locoregional recurrence rates of 16% to 20% have been reported for cases with confirmed tumor-free "noninvolved" surgical margins.[4–6] This suggests that margin determination by white light (WL) examination and confirmation by histopathology alone may be suboptimal. Mindful of the practical difficulties that surgeons encounter while identifying diseased tissue by WL panendoscopy, OSCC surgical success may benefit from visual enhancement of oral tissue abnormality.[7]

Narrow band imaging (NBI; Olympus Medical Systems Corporation, Tokyo, Japan), provides high-resolution enhancement of tissue abnormality through selective wavelength reflectance magnifying endoscopy. Using blue (400–430 nm) and green (525–555 nm) light, NBI highlights both mucosal surface texture and underlying vasculature,[8] facilitating identification of oral neoplasia where angiogenesis is an early feature[9] that can be inconspicuous under conventional WL examination.[10] Diagnostic application of NBI to patients with head and neck cancer benefits their management through improved resection margin assessment,[10] and provides greater diagnostic sensitivity and specificity over other imaging techniques for detection of oral potentially malignant lesions.[8,11]

The purpose of the present study was to provide evidence that NBI surgical margins possess fewer molecular abnormalities than the more conservative WL surgical margins. Accordingly, we performed a prospective bioinformatic evaluation of mRNA expression data for tissue biopsies of tumor core, WL determined margin, and NBI determined margin samples obtained from 18 patients during primary resection of intraoral SCC.

MATERIALS AND METHODS

Ethical consideration and research setting

This study was run in accordance with the Declaration of Helsinki (2008) after approval from the Hospital and

University Human Research Ethics Committees (HREC/ 08/QRBW20 and HREC/10/QRBW336). Patient recruitment and surgical resection occurred between 2010 and 2011 at The Royal Brisbane and Women's Hospital, which hosts a large multidisciplinary head and neck cancer clinic. Laboratory analysis was performed at the University of Queensland Centre for Clinical Research and the Molecular and Clinical Pathology Research Laboratory. Bioinformatic data analysis was performed by the Queensland Facility for Advanced Bioinformatics.

Patient recruitment and sample collection

Eighteen patients with intraoral SCC (which excludes lip, pharynx, and hypopharynx) were enrolled prospectively and provided informed consent. Patient demographics, tumor characteristics, and surgery details are provided as Table 1. Before surgery, primary OSCC sites were visualized under WL and NBI by a consulting physician using an Olympus NBI ENF-VQ nasendoscope with CLV-180 light source and processor (Olympus Medical Systems, Tokyo, Japan). This presurgery inspection was documented by digital video recording and still photographs. On the day of surgery, the surgeon first defined the WL surgical margin based upon WL examination and palpation, then viewed the NBI visualization video and photographs in order to define the NBI surgical margin. Both margins exceeded involved tissue by ≥5 mm in reference to a prior definition of a clear surgical margin.[2,3,7] Only 1 surgeon (M.B.) undertook all WL assessments and resections. OSCC tissue was resected to the NBI-defined surgical margin, then 4-mm punch biopsies were taken from the following zones (see Figure 1): (1) the NBI margin − 5 mm beyond tissue abnormality visible by NBI; (2) the WL margin − 5 mm beyond tissue abnormality visible by WL; and (3) the core of the primary tumor (T) – outside areas of frank ulceration or necrosis.

The exact position of each biopsy was recorded on macroscopic digital photographs of the resected tissue, and then the biopsies were immersed in RNA*later* RNA stabilization solution (Ambion, Life Technologies, Carlsbad, CA) and frozen to −80 °C within 30 minutes from surgery.

RNA isolation

RNA isolation required tissue pulverization in liquid nitrogen and overnight proteinase digestion at 37 °C in 500 μL Buffer RLT (Qiagen, Hilden, Germany) supplemented with 200 ng of Proteinase K (Invitrogen, Life Technologies). RNA isolation from 200 μl lysate used a TRIzol protocol (Invitrogen, Life Technologies) optimized to increase nucleic acid recovery by use of 10 μg glycogen and overnight incubation at −20 °C. DNase treatment used the TURBO DNA-*free* Kit (Ambion, Life Technologies), and then RNA was purified by sodium acetate precipitation. Quality and quantity assessments used a NanoDrop spectrophotometer (Thermo Fisher Scientific, Waltham, MA) and Qubit fluorometer (Invitrogen, Life Technologies). RNA integrity assessment used an Agilent 2100 Bioanalyzer and RNA 6000 Nano kit (Agilent Technologies, Santa Clara, CA).

Gene expression profiling

Microarray utilized GeneChip Human Genome U133 Plus 2.0 Arrays (Affymetrix, Santa Clara, CA) to derive 54 whole genome mRNA expression profiles (NBI, WL, and T samples for 18 patients). Labeled and amplified RNA (aRNA) was generated from 100 ng of total RNA using the GeneChip 3′ IVT Express Kit (Affymetrix) and subject to quality control assessment of size distribution and yield, pre-aRNA and post-aRNA fragmentation using an Agilent 2100 Bioanalyzer before array hybridization.

Bioinformatic analysis in brief

The bioinformatic pipeline achieved the following: (1) quality control and normalization of array data; (2) filtering to remove genes that were not differentially expressed in at least 1 group; (3) identification of pairwise differentially expressed genes; (4) gene ontology annotation; and (5) clustering of differentially expressed genes by principal components analysis (PCA). All reported p values have been adjusted for false discovery rate.

Bioinformatic analysis in detail

Quality control and normalization used affyAnalysisQC[12] and Simpleaffy.[13] Good RNA quality and consistent hybridization quality were evident; however, data from 5 arrays (all NBI margins; patient numbers: 5, 6, 7, 12, and 13) were identified as outliers and excluded. These arrays were identified as outliers on the basis of noncanonical placement in a series of standard quality control plots, such as Normalized Unscaled Standard Error, Relative Log Expression, RNA degradation, and MicroArray plots. The removal of the arrays with poor quality decrease external variability in the dataset and increase the signal to noise ratio, thus improving the statistical power for differential expression testing.

The remaining data (49 samples) were normalized using the GeneChip robust multiarray average normalization method.[14] Preliminary filtering removed probes with coefficients of variation (CV) <0.1 across all arrays, then differential expression of genes was tested using the MANOVA software package via 3 pair-wise comparisons: (1) WL-T; (2) NBI-T; and (3) NBI-WL. A linear model of log-transformed expression data was analyzed by paired one-way analysis of variance adjusted for false discovery rate.[15] Further filtering removed probes that were not differentially expressed in at least 1 group. Pairwise differentially expressed genes were identified from a linear model of log-transformed data using paired t tests with false discovery rate adjustment[15] using the Limma software package.[16] Tumor core expression was the nominal baseline for DE gene interpretation in terms of magnitude and direction for WL and NBI margins. Gene ontology term enrichment used the hypergeometric test in the GOstats software package[17] for the 3 central domains: molecular function (MF), biological process (BP), and cellular component (CC). Gene ontology terms with p values < .05 after false discovery rate adjustment[15] were deemed significantly enriched. All genes that passed the above CV filtering step were used as the background for gene ontology term enrichment. Clustering of differentially expressed genes was achieved by PCA of 38,989

TABLE 1. Study cohort demographic, anatomopathologic, and clinical characteristics.

	Patient details			Environmental risk factors		HPV*	Lesion details							Surgery details			Patient status (postsurgery, y)
ID	Age, y	Sex	Tobacco (PY)	Alcohol			Site	Histology	T	N	M	Stage	Margin	PN or LV invasion	Neck dissection (maximum levels)	Metastatic nodes	
1	83	M	Y (50)	N	-ve		Tongue, dorsal, left	Well differentiated	T4a	N0	MX	IVA	"Close" 1 mm (deep)	None	Unilateral (1, 2, 3)	0/19	Alive; no cancer (4.4)
2	66	M	Y (30)	N	-ve		Floor of mouth, NS	Moderately well differentiated	T4a	N0	MX	IVA	"Clear" >4 mm (lateral)	None	Bilateral (1, 2, 3)	0/45	Alive; no cancer (4.1)
3	64	M	Y (60)	Y	-ve		Floor of mouth, left	Moderately well differentiated	T4a	N2b	MX	IVA	"Clear" 2.5 mm (lateral)	None	Bilateral (1, 2, 3)	2/14	Deceased; metastatic disease† no local recurrence (4.0)
4	64	M	Y (40)	Y	-ve		Floor of mouth, left	Moderately differentiated	T1	N0	MX	I	"Clear" 1.5 mm (deep)	None	None		Alive; no cancer (4.0)
5	53	F	Y (40)	Y	-ve		Floor of mouth, left	Well differentiated	T1	N0	MX	I	"Clear"	None	Unilateral (2, 3, 4)	0/28	Alive; no cancer (4.0)
6	66	F	N	N	-ve		Gingiva, lower, right	Well differentiated	T1	NX	MX	I	"Clear" ≥10 mm (deep, lateral)	None	None		Alive; no cancer (3.8)
7	71	F	Y (10)	N	-ve		Gingiva, lower, anterior	Verrucous carcinoma	T1	NX	MX	I	"Clear" 2 mm (anterior)	None	None		Alive; no cancer (3.7)
8	26	M	N	N	-ve		Tongue, lateral, right	Moderately well differentiated	T4a	N0	MX	IVA	"Clear" 2.1 mm (inferior)	None	Unilateral (1, 2, 3, 4, 5)	0/29	Alive; no cancer (3.6)
9	56	M	Y (25)	Y	-ve		Buccal mucosa, left	Well differentiated	T2	NX	MX	II	"Clear" <5 mm (posterior)	None	None		Alive; no cancer (3.6)
10	75	F	N	N	-ve		Tongue, lateral, right	Well differentiated	T1	N0	MX	I	"Clear" 7 mm (anterior)	None	Unilateral (1, 2, 3)	0/26	Alive; no cancer (3.6)
11	66	M	N	Y	-ve		Hard palate, anterior, left	Moderately well differentiated	TX	NX	MX	I	"Clear" 3.5 mm (anterior)	None	None		Alive; no cancer (3.6)
12	28	M	Y (10)	N	-ve		Floor of mouth, left	Moderately well differentiated	T4a	NX	MX	IVA	"Clear" 4 mm (medial)	None	Unilateral (1, 2, 3)	0/40	Alive; no cancer (3.6)
13	28	F	N	N	-ve		Buccal mucosa, left	Moderately well differentiated	T2	N0	MX	II	"Clear" 4 mm (lateral)	None	Unilateral (1, 2, 3, 4, 5)	0/35	Alive; no cancer (3.5)
14	70	F	N	N	-ve		Buccal mucosa, left	Well differentiated	T4a	NX	MX	IVA	"Clear" 4 mm (posterior)	None	None		Alive; no cancer (3.4)
15	51	M	Y (35)	Y	-ve		Floor of mouth, right	Moderately well differentiated	T4a	N2b	MX	IVA	"Clear" 3.8 mm (lateral)	PN and LV	Bilateral (1, 2, 3)	3/28	Follow-up declined (3.5)
16	62	F	N	N	-ve		Tongue, base, bilateral	Moderately well differentiated	T1	N2b	MX	IVA	"Clear" 2.5 mm (deep)	None	Unilateral (1, 2, 3)	2/28	Alive; no cancer (3.4)
17	54	M	N	N	-ve		Tongue, right	Moderately well differentiated	T4a	N0	MX	IVA	"Clear" 5.9 mm (inferior)	None	Unilateral (1, 2, 3)	0/33	Alive; no cancer (3.4)
18	65	M	Y (40)	N	-ve		Floor of mouth, left	Well differentiated	T1	N0	MX	I	"Clear" 2.5 mm (deep)	None	Bilateral (1, 2, 3)	0/40	Alive; no cancer (3.4)

Abbreviations: PY, pack years; HPV, human papillomavirus; PN, perineural; LV, lymphovascular; –ve, negative; NS, not stated.
Patient details include: study identification number, age in years, and sex. Environmental risk factors: tobacco exposure (PY), alcohol exposure (PY), alcohol exposure, HPV status. Lesion details: anatomic site, histological description, and TNM staging. Surgery details: pathologist statement on margin status and distance to nearest margin, perineural or lymphovascular invasion, details of neck dissection, number of cancer bearing nodes/total number of dissected nodes, patient status at specified time of follow-up.
* HPV status was established using a commercial HPV polymerase chain reaction (PCR) detection set (#6603 TaKaRa Bio, Otsu, Shinga, Japan) for the E6 and E7 regions of HPV-6, 11, 16, 18, 31, 33, 35, 52-b, and 58).
† Distant metastatic disease (mediastinum and lung) diagnosed 1.8 years postsurgery; patient received palliative chemotherapy.
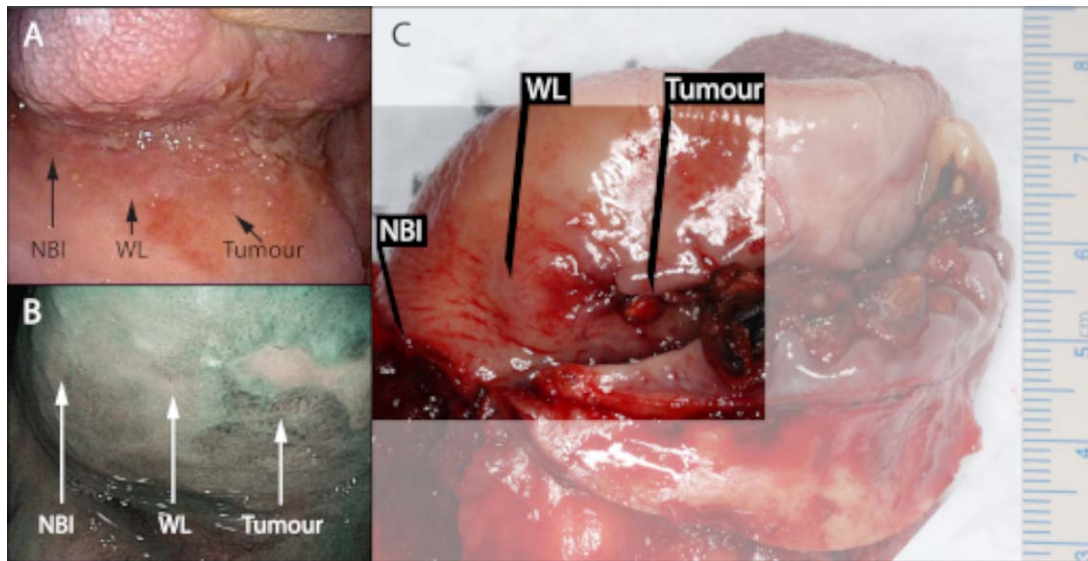
FIGURE 1. Imaging of oral squamous cell carcinoma (OSCC) by white light (WL) panendoscopy (A) and narrow band imaging (NBI) (B). Gross morphology of postsurgical resected tissue (C) – the highlighted area approximates to images A and B. Biopsy sites identified on all images. Patient identification number: 15 (details in Table 1). Structures visible in image C include: lateral tongue, teeth, alveolar process, and buccal vestibule. [Color figure can be viewed in the online issue, which is available at wileyonlinelibrary.com.]

gene probes using the mixOmics software package[18] to process normalized expression data subject only to preliminary filtering to remove probes with CV <0.1 across all arrays. Unsupervised hierarchical clustering and visualization of statistically significant differentially expressed probes used Cluster and Java Treeview software.[19]

Human papillomavirus detection

A human papillomavirus (HPV) Typing Kit[20] (#6603, Takara Shuzo, Ohtsu, Japan) was utilized to detect the presence of HPV using polymerase chain reaction (PCR), in accord with the manufacturer's instructions. The cDNA was synthesized from 500 ng of total RNA from each sample using SuperScript III Reverse Transcriptase kit (Invitrogen, Life Technologies), in accord with the manufacturer's instructions. After cDNA synthesis, HPVpU-1M and HPVpU-31B forward primers were applied in combination with HPVpU-2R reverse primer to amplify malignant (HPV-16, 18, 31, 33, 35, 52-b, and 58) and benign (HPV-6 and 11) HPV subtypes, respectively. Electrophoresis of PCR products was then undertaken using an E-Gel EX 2% Agarose Gel Starter Kit (Invitrogen, Life Technologies). The HPV Typing Set contains 2 pairs of consensus primers designed from the homologous region of the HPV genome to allow the common amplification of the sequence containing E6 and E7 regions (228–268 bp).
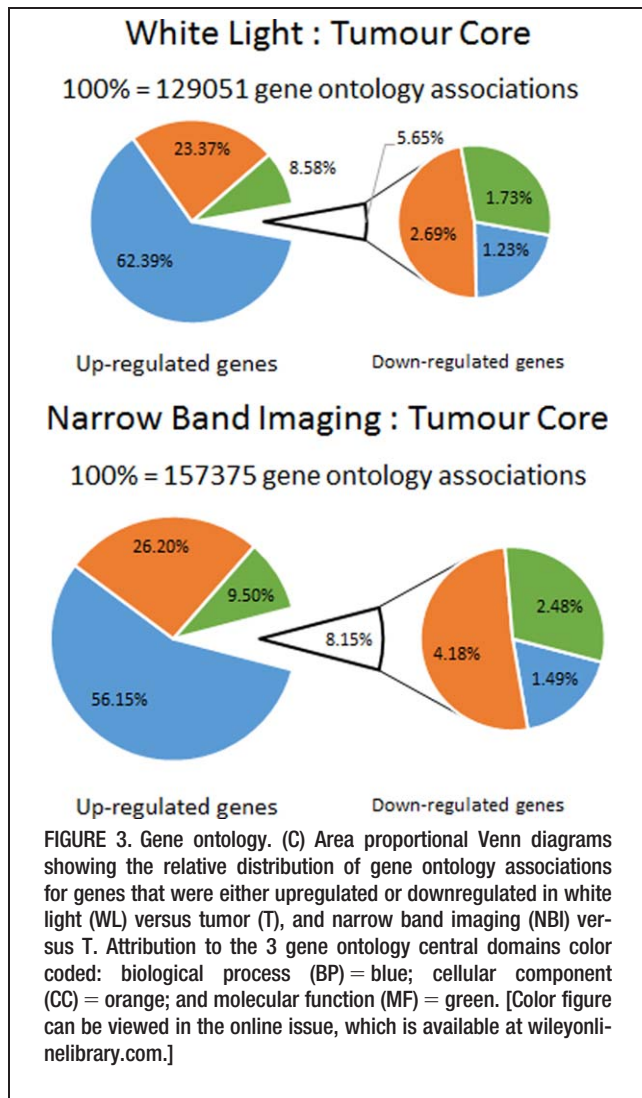
RESULTS

The contextual patient details are presented in Table 1. Age, sex, and patterns of environmental risk factor exposure (tobacco and alcohol intake) exhibited the typical range for patients referred to The Royal Brisbane and Women's Hospital Head and Neck Cancer clinic. All tumor biopsies were negative for HPV. Neck dissection was indicated for the majority (12) of patients, although only 3 presented metastatic nodes. Tumor histology was predominantly moderate (10) to well (7) differentiated OSCC, with 1 case of verrucous carcinoma. Independent histopathology indicated "clear" margins for all but 1 resection, although only 2 had margins with >5 mm separation from disease. One "close" margin had just 1 mm of separation. Note that tissue shrinkage was not accounted for in these margin assessments.[7] The most current follow-up data (3.4–4.4 years postsurgery) is presented in Table 1. Barring one, all patients were alive and, except for 1 patient who declined follow-up, none have had local cancer recurrence.

Whole genome mRNA expression data from 54 arrays were processed. These comprised 3 tissue samples, tumor, WL, and NBI, from each of 18 patients. Quality control procedures eliminated data from 5 arrays (patient numbers: 5, 6, 7, 12, and 13), all of which were NBI tissue samples. After normalization and removal of probes with low coefficients of variation, 38,989 probes entered the bioinformatics pipeline.

A total of 7633 probes, representing 4794 genes (Gene Symbols), were differentially expressed significantly in one or more of the 3 tissue groups (paired t test with adjusted p values $< .01$). In terms of the number of differentially expressed genes, greater molecular divergence was seen between NBI and tumor sites (4387 DE genes) than between WL and tumor sites (3266 DE genes). Molecular divergence was not apparent between NBI and WL with no differentially expressed genes reported.

Clustering of differentially expressed genes by PCA identified a discriminatory component that separated tumor from the WL and NBI samples (Figure 2A). Although PCA clustering did not fully segregate WL

FIGURE 2. Bioinformatic results. (A) Principal component analysis (PCA) plot. (B) Unsupervised hierarchical clustering of differentially expressed probes (split and abridged heat map). Both plots are annotated with patient identification number (Table 1) and a color code to indicate biopsy location: red = tumor core (T); green = white light (WL); blue = narrow band imaging (NBI). [Color figure can be viewed in the online issue, which is available at wileyonlinelibrary.com.]

from NBI samples, the PCA plot placed most WL samples between NBI and tumor samples (Figure 2A). The trend, therefore, was for the discriminatory component to segregate tumor, WL, and NBI tissue biopsies appropriately along the tumor to normal tissue axis based solely upon their mRNA profiles.

An unsupervised hierarchical clustering of the statistically significant differentially expressed probes defined a primary partition between the mRNA profiles of tumor samples and nontumor samples (NBI and WL; Figure 2B). Importantly, 4 of 18 WL samples (22%) clustered with the tumor samples, whereas none of the NBI samples clustered with the tumor side of the primary partition (Figure 2B). The 4 WL samples that clustered alongside the tumor group came from patient numbers: 1, 7, 10, and 11. Of these, only 1 sample (patient 7-WL) was not complemented by its matched NBI sample, the data having failed quality control.

Gene ontology enrichment was performed for the 4794 differentially expressed genes. The total numbers of gene ontology associations to attain statistical significance ($p < .05$; false discovery rate adjusted) was 18% larger for NBI (157,375) than for WL (129,051); each group being referenced to the tumor core. Note that individual genes can have multiple gene ontology associations. Figure 3 presents the numbers of gene ontology associations split by the direction of regulation and organized into the 3 gene ontology central domains: MF, BP, and CC. Not surprisingly, the overall distribution of gene ontology associations over the 3 central domains was broadly similar for both NBI and WL when referenced to tumor core. BP was the most highly represented, classifying 58% and 64% of gene ontology associations for NBI and WL, respectively. The BP domain encompasses: cell cycle, development, metabolic processes, regulation, signaling, and much more. Broadly, the CC domain details the cell,

FIGURE 3. Gene ontology. (C) Area proportional Venn diagrams showing the relative distribution of gene ontology associations for genes that were either upregulated or downregulated in white light (WL) versus tumor (T), and narrow band imaging (NBI) versus T. Attribution to the 3 gene ontology central domains color coded: biological process (BP) = blue; cellular component (CC) = orange; and molecular function (MF) = green. [Color figure can be viewed in the online issue, which is available at wileyonlinelibrary.com.]

its membranes, and associated receptors, and, in this study, classified 38% and 26% of gene ontology associations for NBI and WL, respectively. The MF domain, which groups the effector modalities such as noncovalent binding, enzyme activity, receptor activity, or transporter activity, accounted for 12% and 10% of gene ontology associations for NBI and WL, respectively. Interestingly, the vast majority (92% and 94% for NBI and WL, respectively) of gene ontology associations were for genes that were downregulated in the tumor core (see Figure 3).

DISCUSSION

This study of 18 patients with intraoral SCC used gene expression profiling and bioinformatics to evaluate the molecular divergence between the tumor core and adjacent surgical resection margins established by conventional WL examination or by selective wavelength reflectance enhanced magnifying endoscopy (NBI). The results provide evidence that the surgical margins determined by NBI possess fewer molecular abnormalities than the more conservative surgical margins determined by WL examination. This finding provides molecular foundation to our previously reported clinical evaluation

of NBI[10] and supports our hypothesis that resection to surgical margins that are determined by NBI rather than by WL examination leave less potentially malignant residual tissue and thereby increase the likelihood of successful ablative surgery.

Involved surgical margins (exhibiting malignant or dysplastic pathology at or close to the inked resection margin) have been shown to increase the risk of death at 5 years by 90% in a cohort of 707 patients with intraoral SCC for whom 14.6% of surgical resections produced involved margins.[4] The reported incidence of involved margins for head and neck cancer resections varies greatly, largely because of inconsistency in the definition of an involved margin.[3,4,7] The balance of opinion includes carcinoma in situ, but excludes dysplasia from this definition, and defines "close" margins as having involvement within 5 mm of the inked margin.[3,7] The use of such arbitrary and nonstandardized criteria for determining such a highly valued measure of surgery success is extraordinary. It is at odds with emerging clinical evidence that places much higher weighting to the presence of dysplasia for the prognostic evaluation of oral potentially malignant lesions,[21] and is at odds with evidence of a continuum of molecular aberrations along the spatiotemporal axis of malignant transformation.[22] Similarly, the exhibited confidence in histopathological discrimination of carcinoma in situ from dysplasia (to include one but exclude the other from the definition of an involved margin) is also surprising in light of the widely acknowledged inconsistency in such diagnoses[23–25] and in the grading of dysplasia.[26–28] Analysis of biomarker profiles that reflect the cumulative genetic and epigenetic aberrations that accompany oral neoplastic transformation may eventually supplant our current reliance on diagnostic histopathology.[22] In this regard, molecular assessment of surgical margins has the marked advantage of observing the locoregional genetic instability[29] that undoubtedly contributes to localized postexcisional cancer recurrence independently of noninvolvement of the surgical margins.

Of the 4794 differentially expressed genes identified here, 1121 less genes were differentially expressed in tumor relative to WL (3266 DE genes) than in tumor relative to NBI tissues (4387 DE genes). This 25.6% greater molecular divergence between tumor and NBI margins than between tumor and WL margins is perhaps the most important finding of the study. It puts a number to the extent to which NBI-defined surgical margins were placed within less involved tissue than would have been the case for conventionally assigned WL surgical margins in this cohort of 18 patients with intraoral SCC. The strength of this finding lies in its objectivity. Unsupervised genome wide mRNA expression profiling generates data that is uncompromised by interobserver and intraobserver variability that can influence conventional histopathology,[23–28] and may be less prone to the subjective interpretation that has been documented for conventional assessment of surgical margin involvement.[3,4]

PCA identified a discriminatory component that separated tumor from WL and NBI samples and, although the WL and NBI samples were not fully resolved, the PCA plot aligned the tumor, WL, and NBI tissue biopsies appropriately along the tumor to normal tissue axis based

solely upon their mRNA profiles. This important observation indicates that a pattern exists within the mRNA profiles of our study cohort that can identify the degree of molecular abnormality at biopsy sites radiating out from the tumor core. Crucially, the biopsy sites were not arbitrarily selected, rather they were from within WL-designated "normal" tissue and NBI-designated "normal" tissue. Therefore, PCA analysis strongly supports our view that resection to surgical margins determined using NBI rather than WL will leave less molecularly abnormal residual tissue. Furthermore, unsupervised hierarchical clustering of the differentially expressed probes defined a partition between the mRNA profiles of tumor samples and nontumor samples (NBI and WL). Importantly, 4 of 18 WL samples (22%) clustered with the tumor samples, whereas none of the NBI samples clustered with the tumor samples. This implies that 22% of the surgical procedures in this study directly benefited from the use of NBI to define the surgical margins.

Gene ontology enhancement uses various statistical approaches (in this case, hypergeometric modeling) to assign biological context to lengthy lists of differentially expressed genes. The output draws upon an actively maintained database of empirically inferred gene process annotations (in this case, the MetaCore database; Thomson Reuters Corporation) and is not weighted for the observed magnitude of differential regulation. In this study, the total number of statistically significant gene ontology associations was 18% larger for NBI than for WL, which is partially a consequence of the 25.6% larger number of differentially expressed genes for NBI than for WL. Not surprisingly, the distribution of gene ontology associations over the 3 central domains was similar for both NBI and WL samples, in order of prevalence: $BP > CC > MF$. Interestingly, the majority of the gene ontology association involved genes were downregulated in the tumor core. This predominance of gene downregulation in tumor core is expected because neoplasia causes a reduction in the overall tissue complexity by repressing normal patterns of differentiation. Lost regulation of cell cycling produces the most conspicuous pathologic characteristics of tumors: hyperproliferation with impaired and dysregulated cellular differentiation. Consequent partial loss (well differentiated OSCC) or complete loss (poorly differentiated OSCC) of normal tissue hierarchy deprives tumors of the breadth of mRNA expression that is present in normal tissues bearing defined regions of cellular proliferation and differentiation. Taken together, the gene ontology association data presented in Figure 3 portrays a pattern of increasing cell phenotypic diversity at biopsy sites radiating out from the tumor core, this phenotypic diversity being influenced by both the overall numbers of differentially expressed genes and the breadth of their molecular actions.

This study applied gene expression profiling and bioinformatic techniques to evaluate molecular divergence between tissue biopsies ranging from the tumor core to surgical resection margins established by conventional WL examination or by NBI. Ultimately, PCA and unsupervised clustering of differentially expressed genes identified 4 resections for which the WL biopsies possessed greater molecular similarity to tumors than to NBI tissues.

The 4 respective patients (22% of the study cohort) benefited directly from use of NBI to determine their surgical margins. Overall, the results portray a pattern of decreasing molecular abnormality with distance from the tumor core that crosses the WL defined surgical margin. This finding provides molecular foundation to our hypothesis that resection to surgical margins that are determined by NBI rather than by WL examination will leave less potentially malignant residual tissue and thereby increase the likelihood of surgical success. We infer that resection to NBI-defined margins will leave less dysplastic and malignant residual tissue and will increase surgical success rates, and we advocate greater uptake of NBI for establishing surgical margins for OSCC resections.

Acknowledgments

REFERENCES

1. Warnakulasuriya S. Global epidemiology of oral and oropharyngeal cancer. *Oral Oncol* 2009;45:309–316.
2. Kurita H, Nakanishi Y, Nishizawa R, et al. Impact of different surgical margin conditions on local recurrence of oral squamous cell carcinoma. *Oral Oncol* 2010;46:814–817.
3. Meier JD, Oliver DA, Varvares MA. Surgical margin determination in head and neck oncology: current clinical practice. The results of an International American Head and Neck Society Member Survey. *Head Neck* 2005; 27:952–958.
4. Binahmed A, Nason RW, Abdoh AA. The clinical significance of the positive surgical margin in oral cancer. *Oral Oncol* 2007;43:780–784.
5. González–García R, Naval–Gías L, Román–Romero L, Sastre–Pérez J, Rodríguez–Campo FJ. Local recurrences and second primary tumors from squamous cell carcinoma of the oral cavity: a retrospective analytic study of 500 patients. *Head Neck* 2009;31:1168–1180.
6. Yanamoto S, Yamada S, Takahashi H, et al. Clinicopathological risk factors for local recurrence in oral squamous cell carcinoma. *Int J Oral Maxillofac Surg* 2012;41:1195–1200.
7. Hinni ML, Ferlito A, Brandwein–Gensler MS, et al. Surgical margins in head and neck cancer: a contemporary review. *Head Neck* 2013;35:1362–1370.
8. Bhatia N, Lalla Y, Vu AN, Farah CS. Advances in optical adjunctive AIDS for visualisation and detection of oral malignant and potentially malignant lesions. *Int J Dent* 2013;2013:194029.
9. Fujii S, Yamazaki M, Muto M, Ochiai A. Microvascular irregularities are associated with composition of squamous epithelial lesions and correlate with subepithelial invasion of superficial-type pharyngeal squamous cell carcinoma. *Histopathology* 2010;56:510–522.
10. Nguyen P, Bashirzadeh F, Hodge R, et al. High specificity of combined narrow band imaging and autofluorescence mucosal assessment of patients with head and neck cancer. *Head Neck* 2013;35:619–625.
11. Vu AN, Farah CS. Efficacy of narrow band imaging for detection and surveillance of potentially malignant and malignant lesions in the oral cavity and oropharynx: a systematic review. *Oral Oncol* 2014;50:413–420.
12. Eijssen LM, Jaillard M, Adriaens ME, et al. User-friendly solutions for microarray quality control and pre-processing on ArrayAnalysis.org. *Nucleic Acids Res* 2013;41(Web Server issue):W71–W76.
13. Wilson CL, Miller CJ. Simpleaffy: a BioConductor package for Affymetrix Quality Control and data analysis. *Bioinformatics* 2005;21:3683–3685.
14. Wu Z, Irizarry RA. Preprocessing of oligonucleotide array data. *Nat Biotechnol* 2004;22:656–658; author reply 658.
15. Benjamini Y, Hochberg Y. Controlling the false discovery rate: a practical and powerful approach to multiple testing. *J R Stat Soc Series B Stat Methodol* 1995;57:289–300.
16. Smyth GK. Linear models and empirical Bayes methods for assessing differential expression in microarray experiments. *Stat Appl Genet Mol Biol* 2004;3:Article3.

17. Falcon S, Gentleman R. Using GOstats to test gene lists for GO term association. *Bioinformatics* 2007;23:257–258.
18. Lê Cao K, González I, Déjean S. integrOmics: an R package to unravel relationships between two omics datasets. *Bioinformatics* 2009;25: 2855–2856.
19. Eisen MB, Spellman PT, Brown PO, Botstein D. Cluster analysis and display of genome-wide expression patterns. *Proc Natl Acad Sci U S A* 1998; 95:14863–14868.
20. Fujinaga Y, Shimada M, Okazawa K, Fukushima M, Kato I, Fujinaga K. Simultaneous detection and typing of genital human papillomavirus DNA using the polymerase chain reaction. *J Gen Virol* 1991;72(Pt 5): 1039–1044.
21. Dost F, Lê Cao KA, Ford PJ, Farah CS. A retrospective analysis of clinical features of oral malignant and potentially malignant disorders with and without oral epithelial dysplasia. *Oral Surg Oral Med Oral Pathol Oral Radiol* 2013;116:725–733.
22. Lingen MW, Pinto A, Mendes RA, et al. Genetics/epigenetics of oral premalignancy: current status and future research. *Oral Dis* 2011;17 Suppl1:7–22.
23. Pindborg JJ, Reibel J, Holmstrup P. Subjectivity in evaluating oral epithelial dysplasia, carcinoma in situ and initial carcinoma. *J Oral Pathol* 1985; 14:698–708.
24. Karabulut A, Reibel J, Therkildsen MH, Praetorius F, Nielsen HW, Dabelsteen E. Observer variability in the histologic assessment of oral premalignant lesions. *J Oral Pathol Med* 1995;24:198–200.
25. Reibel J. Prognosis of oral pre-malignant lesions: significance of clinical, histopathological, and molecular biological characteristics. *Crit Rev Oral Biol Med* 2003;14:47–62.
26. Brothwell DJ, Lewis DW, Bradley G, et al. Observer agreement in the grading of oral epithelial dysplasia. *Community Dent Oral Epidemiol* 2003;31:300–305.
27. Lumerman H, Freedman P, Kerpel S. Oral epithelial dysplasia and the development of invasive squamous cell carcinoma. *Oral Surg Oral Med Oral Pathol Oral Radiol Endod* 1995;79:321–329.
28. Abbey LM, Kaugars GE, Gunsolley JC, et al. Intraexaminer and interexaminer reliability in the diagnosis of oral epithelial dysplasia. *Oral Surg Oral Med Oral Pathol Oral Radiol Endod* 1995;80:188–191.
29. Jessri M, Farah CS. Next generation sequencing and its application in deciphering head and neck cancer. *Oral Oncol* 2014;50:247–253.